Enlargement of Interscapular Brown Adipose Tissue in Growth Hormone Antagonist Transgenic and in Growth Hormone Receptor Gene-Disrupted Dwarf Mice

YUESHENG LI ,[1]*† JOANNE R. KNAPP,§ AND JOHN J. KOPCHICK [2],*‡

*Edison Biotechnology Institute, †Molecular and Cellular Biology Program, Department of Biological Sciences, and ‡Department of Biomedical Sciences, College of Osteopathic Medicine, Ohio University, Athens, Ohio 45701; and §Department of Animal Sciences, University of Vermont, Burlington, Vermont 05405

Growth hormone (GH) acts on adipose tissue by accelerating fat expenditure, preventing triglyceride accumulation, and facilitating lipid mobilization. To investigate whether GH is involved in the development and metabolism of interscapular brown adipose tissue (BAT), a site of nonshivering thermogenesis, we employed three lines of transgenic mice. Two of the lines are dwarf due to expression of a GH antagonist (GHA) or disruption of the GH receptor/binding-protein gene. A third mouse line is giant due to overexpression of a bovine GH (bGH) transgene. We have found that the body weights of those animals are proportional to their body lengths at 10 weeks of age. However, GHA dwarf mice tend to catch up with the nontransgenic (NT) littermates in body weight but not in body length at 52 weeks of age. The increase of body mass index (BMI) for GHA mice accelerates rapidly relative to controls as a function of age. We have also observed that BAT in both dwarf mouse lines but not in giant mice is enlarged in contrast to nontransgenic littermates. This enlargement occurs as a function of age. Northern analysis suggests that BAT can be a GH-responsive tissue because GHR/BP mRNAs were found there. Finally, the level of uncoupling protein-1 (UCP1) RNA was found to be higher in dwarf mice and lower in giant animals relative to controls, suggesting that GH-mediated signaling may negatively regulate UCP1 gene expression in BAT. Exp Biol Med 228:207–215, 2003

Key words: growth hormone antagonist; growth hormone receptor/binding-protein gene disruption; brown adipose tissue; uncoupling protein-1, obesity

Adipose tissues are one of many targets for growth hormone (GH) action. GH has been shown to accelerate fat expenditure, prevent triglyceride accumulation, and facilitate lipid mobilization (1). In the "GH-fat cycle" model (2), a reduction in GH's lipolytic effect is postulated to result in an accumulation of body fat. In obese animals, GH output is reduced due primarily to hypothalamic disorders. In fact, GH secretion patterns are markedly reduced in obese compared with normal-weight men (3). Also, GH therapy reduces abdominal fat mass in abdominally obese men (4) and in a site-specific manner in GH-deficient, obese children (5). Moreover, GH significantly decreases the activity of lipoprotein lipase (LPL) and increases the activity of hormone-sensitive lipase (HSL) in adipose tissues and adipocytes (6, 7).

There are two types of adipose tissues: brown adipose tissue (BAT) and white adipose tissue (WAT). WAT is yellowish-white and stores energy in the form of lipid, whereas BAT is reddish-brown and has higher metabolic activity per cell than WAT. BAT has a large quantity of mitochondria with abundant cytochromes and a rich capillary bed that supplies "fuel" and oxygen (8). Hence, BAT is a site of heat production that has been termed nonshivering thermogenesis.

Adipose tissues are large aggregates of adipocytes. Their lineage is derived from a multipotent stem cell population of mesodermal origin that can also develop into muscle and cartilage (9). Brown adipocytes are smaller than white adipocytes and their cytoplasm contains multiple noncoalescent lipid droplets of varying size. Thus, a predominant difference between BAT and WAT is the number of lipid droplets in adipocytes (10). Also, a distinct molecular feature between these cells is the presence of a mitochondria thermogenic proton conductance pathway that includes uncoupling protein-1 (UCP1) in BAT.

UCPs are a family of membrane proteins that generate

This study was supported in part by the State of Ohio's Eminent Scholar's Program, which includes a grant from Milton and Lawrence Goll.

[1] Current address: Department of Neurosurgery, University of Virginia Health System, Cobb Hall Room 2028, Charlottesville, VA 22908-0420.

[2] To whom requests for reprints should be addressed at Edison Biotechnology Institute, Konneker Research Laboratories, Room 206A, Ohio University, Athens, OH 45701-2979. E-mail: kopchick@ohiou.edu

Received April 1, 2002.
Accepted October 16, 2002.

1535-3702/03/2282-0207$15.00

heat by uncoupling the mitochondrial electron transport chain. UCP1 is the best-characterized protein in this family and is expressed at relatively high levels in BAT (11). Recent studies have shown that UCP1 is not exclusively expressed in BAT (12, 13). Also, its proton transport activity can be activated by free fatty acids and inhibited by purine nucleotides (8). UCP1 also can be regulated by physiological stimuli such as cold stress. Its importance was shown in UCP1-DTA (diphtheria toxin A-chain) transgenic mice where the mice were found to be BAT deficient and were hyperphagic or obese (14). Also, aP2-UCP1 transgenic mice that overexpressed UCP1 in WAT were resistant to obesity (15). Additionally, UCP1 gene-disrupted mice possess a nonobese phenotype and were ambient temperature sensitive (16, 17).

In addition to UCP1 protein, other UCP family members have been identified. UCP2 is ubiquitously expressed (18). UCP3 is specifically found in skeletal muscle in humans, but in both muscle and BAT in rodents (19), and UCP4 is exclusively expressed in brain (20). In adipose tissues, expression of UCP2 mRNA and probably UCP3 mRNA are correlated with the change of energy expenditure (21, 22).

In this report, we show that GH-mediated signaling plays an important role in BAT development and thermal regulation. We used two lines of transgenic dwarf mice: GH antagonist (GHA) and GH receptor/binding-protein (R/BP) gene-disrupted (knockout, KO) mice, and one line of transgenic giant mice expressing bovine (b) GH. We found that GHR and GHBP mRNAs were detectable in BAT. We also observe abnormal enlargement of BAT in both GHA and GHR/BPKO mice, but not in bGH mice. We also report that GH signaling downregulates UCP1 gene expression in BAT.

Materials and Methods

Animals. In this study, the GH or GHA transgenic or GHR knockout mice were homozygous for the altered gene. The growth phenotypes of the mice have been discussed previously (23–30). In bGH and GHA mice, one to five transgene copies were incorporated into the genome. They were generated by breeding a single transgenic male mouse expressing one of the specific mutations with nontransgenic (NT) C57BL/6 female mice. Because a single transgenic male expressing each of the mutations was used for breeding, the number of transgene insertions in all subsequent offspring was uniform. Expression of a transgene encoding either bGH or GHA was directed by mouse metallothionein I transcriptional regulatory region. bGH mice have serum bGH levels ranging between 0.2 and 6.0 μg/ml, whereas GHA mice that overexpress bGH-G119K maintain serum GHA levels of approximately 5 μg/ml (24, 28, 30). GHR/BP KO homozygous ($GHR/BP^{-/-}$) mice that lack mGHR and mGHBP were also backcrossed onto a C57BL/6 background (29). NT litter mates from each of the groups served as controls. All mice were fed *ad libitum* with rodent chow (5004; Ralston-Purina, St. Louis, MO) and were housed under standard environmental conditions. One hundred fifty-two mice were used in this study with the breakdown as follows: 9 bGH male and 11 NT male littermates; 3 GHA female and 6 NT female littermates; 41 GHA male and 52 NT male littermates; and 15 $GHR/BP^{-/-}$ male and 15 $GHR/BP^{+/+}$ male littermates. The Ohio University IACUC approved all procedures and protocols.

Total RNA Preparations. Interscapular adipose tissues (iAT) consist of peripheral yellowish-white fat and central reddish-brown fat. The features that distinguished iBAT from iWAT were tissue color and the presence or absence of UCP-1 RNA. To determine the heterogeneity of adipocytes in iAT in terms on iBAT and iWAT, the tissues were separately dissected, weighed, and the levels of UCP-1 were determined. Note that UCP-1 is highly expressed in BAT. Subcutaneous WAT (scWAT), gonadal WATs that include epididymal WAT (eWAT) and ovarian WAT (oWAT), liver, and kidneys were also removed and weighed. All tissues were placed in 10 volumes of cold RNA STAT-60 reagent (TEL-TEST, Friendswood, TX) and were carefully homogenized on ice. RNA was prepared following the manufacture's protocol and was stored in 75% ethanol at –80°C.

Polymerase Chain Reaction (PCR) Probe Labeling. Oligonucleotides shown in Table I were used to generate DNA probes from plasmid DNAs encoding β-actin, mGHBP, or UCP_1 (a gift from Dr. Leslie P. Kozak, The Jackson Laboratory, Bar Harbor, ME) (11) following the PCR amplification protocol in the Advantage-HF 2 PCR Kit (Clontech, Palo Alto, CA). These PCR products then served as templates in the secondary asymmetric PCR amplification in which only antisense strand primers were used for probe labeling. The amplification parameters were as follows: 95°C for 30 sec, 35 cycles of 95°C for 10 sec, and 68°C for 2 min. All products were resolved by 1% agarose

Table I. Sets of Primers for Specific cDNA Synthesis

Specific mRNA	A set of primers	Size of fragment (bp)
β-actin	(+) 5′-TGTCAGGTCTTCTTAACCTTGG-3′ (–) 5′-CCACGAATCCCGGTCAAACTAATGT-3′	540
GHR/BP	(+) 5′-GCCAGGCTTCCAGTACCATT-3′ (–) 5′-GGTACTGTCCTGGCAGAGAGTT-3′	522
UCP1	(+) 5′-GCCAGGCTTCCAGTACCATT-3′ (–) 5′-GGTACTGTCCTGGCAGAGAGTT-3′	605

gel electrophoresis and were subsequently purified using a QIAEX II Agarose Gel Extraction kit (Qiagen, Chatsworth, CA).

For PCR-digoxigenin (Dig) probe labeling, a probe synthesis mixture containing 0.1 p*M* dig-11-dUCP, was added in PCR buffer to 0.2 p*M* antisense strand primer, 0.4 p*M* dTTP, and 0.5 p*M* each of dATP, dCTP, and dGTP, 0.1 ng of PCR-amplified DNA fragment, and 0.4 μl of Advantage-HF 2 Polymerase mix (Clontech) in a total volume of 20 μl following the instructions found in the PCR DIG Probe Synthesis kit (Roche, Indianapolis, IN). The concentration of PCR-Dig-labeled probe used was as described in the Genius System User's Guide for labeling (Roche).

For preparation of the PCR-^{32}P-labeling probe, 20 μCi each of [α^{32}P]dCTP and [α^{32}P]dTTP was mixed with 20 n*M* each of dATP and dGTP, PCR buffer, 0.2 p*M* antisense strand primer, 0.1 ng of PCR-amplified DNA fragment, and 0.4 μl Advantage-HF 2 Polymerase mix in total volume of 20 μl following the protocols in the StripAble PCR probe Synthesis kit (Ambion, Austin, TX). Unincorporated radionucleotides were removed by gel filtration using STE SELECT-D G-25 columns (Eppendorf-5 Prime, Boulder, CO). Probe-specific activities were determined using a Multi-Purpose Scintillation Counter (LS 6500; Beckman Instruments, Fullerton, CA).

Northern Analysis. Total RNA samples were resolved by 1% formaldehyde/agarose gel electrophoresis, subsequently transferred overnight to a positively charged nylon membrane (Roche), cross-linked to the membrane in a UV Stratalinker oven (Stratagene, La Jolla, CA), prehybridized with either DIG Easy Hyb solution (Roche) or freshly made prehybridization buffer (6× SSPE, 5× Denhardt's Reagent, 0.5% SDS, 1.0 mg/ml salmon sperm DNA, and 50% deionized formamide) at 50°C for 1 hr, and then hybridized with either 10 ng/ml PCR Dig-labeled or 1×10^6 cpm/ml PCR ^{32}P-labeled probes in a Micro Hybridization Incubator (model 2000; Robbins Scientific, Sunnyvale, CA) at 50°C for 16 hr. Washing procedures and detection of Dig-labeled nucleic acids were as described in the Genius System User's Guide (Roche). For detection of ^{32}P-labeled nucleic acids, membranes were washed once with 1× SSC/0.1% SDS at room temperature for 20 min and three times with 0.2× SSC/0.1% SDS at 68°C for 20 min, subsequently wrapped, exposed to film (Bio-Max MR; Eastman-Kodak Company, Rochester, NY), and developed using a film processor (SRX-101 Medica; Konica Corporation, Tokyo, Japan). Film exposure times varied from sample to sample. For detection of ^{32}P-labeled nucleic acids, films were exposed at –80°C. All images of Northern blots were scanned using a scanner (Agfa Duoscan T1200; Agfa, Ridgefield Park, NJ) installed with fotolook PS 3.05 (Agfa) and Adobe Photoshop 4.0.1 software (Adobe Systems, Mountain View, CA). The intensity volumes of individual signals were determined using Molecular Analyst, version 2.1.2 software (Bio-Rad Laboratories, Hercules, CA) and were compared with control levels.

Statistical Analysis. One-way analysis of variance (ANOVA) was applied to compare a single effect of genotype (bGH, GHA, or GHR/BP$^{-/-}$ mice versus NT littermates) as a function of either gender or age. Two-way ANOVA was also used to compare the primary effect of genotype (bGH, GHA, or GHR/BP$^{-/-}$ mice versus NT littermates) plus the secondary effect of age (10 to 52 weeks) and gender. The program STATISTICA 6.0 (StatSoft, Tulsa, OK) was used in this study.

Results

GH-Mediated Signaling Plays an Important Role in Body Weight. The growth patterns of transgenic mice were significantly altered from those of NT littermates (Table II). At 10 weeks of age, bGH mice were large and had a growth ratio of 117.5% ± 10.8% relative to their NT littermates. In contrast, GHA mice were dwarf with a growth ratio of 66.2% ± 7.6% relative to male NT littermates and 66.4% ± 2.9% relative to female NT littermates. Sex differences in terms of body weight ($P < 0.01$) in both GHA and NT groups also were observed. Disruption of the GHR/BP gene severely hindered body growth ($P < 0.01$) in GHR/BP$^{-/-}$ mice with a growth ratio of 51.8% ± 11.6% relative to GHR/BP$^{+/+}$ animals ($n = 7$). These observations were consistent with data previously reported (23–30).

Although the body weight was significantly different ($P < 0.01$) between 10 to 52 weeks of age between GHA and the NT groups, the differences gradually diminished ($P = 0.233$) as a function of age. The weights of GHA mice approached 94.6% ± 9.0% of those of NT littermates at 52 weeks of age, with no significant change of body length from nose to anus (Table II). Thus, they were "fatter." These observations agree with previous reports (30). Because body mass index (BMI) is defined as a ratio of body weight to a square of body length, GHA mice have a greater BMI than do NT littermates.

iAT Lobes Are Abnormally Enlarged in GHA and GHR/BPKO Mice. We observed that iAT lobes were enlarged in all GHA and GHR/BP$^{-/-}$ mice in contrast to control animals at 10 weeks of age. When comparing male GHA mice with their NT littermates, a tissue enlargement ($P < 0.01$) occurred in iAT, including both iBAT and iWAT. Such enlargements were more pronounced ($P << 0.01$) when tissue weight was normalized to body weight (Table III). Like male GHA mice, female GHA animals had similar tissue enlargement profiles ($P < 0.01$) in both iBAT and iWAT when normalized to animal weight.

When comparing GHR/BP$^{-/-}$ to GHR/BP$^{+/+}$ mice, significant increases of normalized iBAT and iWAT components were apparent in GHR/BP$^{-/-}$ mice ($P < 0.01$). However, normalization of tissue weight by body weight did not reveal a significant difference in iBAT and iWAT between bGH mice and their NT littermates (Table III), suggesting that the growth of iAT lobes is proportional to body weight in bGH mice.

Table II. Body Weight and Growth Rate (GR) of Transgenic (TG) Mice

Group	Age (weeks)	Sex	TG mice	Body weight ± SEM	(N)	*P*	GR (%) ± SEM	(n)
A	10	M	GHR/BP −/−	13.780 ± 2.006	(15)	0.000[a]	51.8 ± 11.6	(7)
B	10	M	GHR/BP +/+	29.033 ± 3.600	(15)			
C	10	F	GHA	13.733 ± 0.802	(3)	0.000[b]	66.4 ± 2.9	(2)
D	10	F	NT	20.583 ± 1.053	(6)	0.000[c]		
						0.001[d]		
E	10	M	GHA	17.693 ± 1.862	(30)	0.000[e]	66.2 ± 7.6	(21)
F	10	M	NT	26.337 ± 2.136	(41)	0.000[f]		
						0.000[g]		
G	52	M	GHA	40.673 ± 6.176	(11)	0.233[h]	94.6 ± 9.0	(6)
H	52	M	NT	43.709 ± 5.378	(11)			
I	10	M	bGH	31.833 ± 2.860	(9)	0.000[i]	117.5 ± 10.8	(4)
J	10	M	NT	26.091 ± 1.301	(11)			

Note. N = number of subjects; n = number of pairs of subjects; *P* values = calculated by one-way ANOVA analysis (STATISTICAL).
[a] A vs B.
[b] C vs D.
[c] D vs F.
[d] C vs E.
[e] E vs F.
[f] F vs H.
[g] E vs G.
[h] G vs H.
[i] I vs J.

iAT Lobes Are Enlarged As a Function of Age in GHA Mice. The iAT lobes were larger in weight and lighter in appearance, whereas scWAT pads were thicker at 52 weeks of age than those at 10 weeks of age in both GHA mice and their NT littermates. When comparing mice at 10 to 52 weeks of age, we noticed a significant difference in iAT, iBAT, iWAT, and eWAT weights (*P* ranging from 0.001 to 0.021) in both GHA mice and NT littermates (Table III). The only exception was in the normalized iWAT weight ($P = 0.136$) found in NT mice. These data indicated that the weight of iWAT may more likely increase with that of iAT lobes in GHA mice during growth.

As mentioned above, 10-week-old GHA mice had significantly enlarged iBAT and iWAT. At 52 weeks of age, GHA mice still possessed a statistical difference in iAT lobes ($P = 0.025$) and iWAT ($P = 0.022$) but not in iBAT ($P = 0.127$) when comparing normalized tissue weights with those of NT littermates (Table III). These data suggest that iBAT expansion may slow down in GHA mice whose weights catch up to that of NT littermates as a function of age.

When comparing male and female GHA mice at 10 weeks of age, a statistical difference was found in iBAT ($P < 0.01$), but not in the other tissues analyzed (Table III).

Table III. Normalization of Adipose Tissue Weights by Body Weights in Dwarf and Giant Mice

Group	Age (weeks)	Sex	Transgenic mice	iBAT			iWAT			iAT			eWAT		
				R(%) ± SEM	(N)	*P*	R(%) ± SEM	(N)	*P*	R(%) ± SEM	(N)	*P*	R(%) ± SEM	(N)	*P*
A	10	M	GHR/BP −/−	7.143 ± 2.304	(15)	0.000[a]	8.164 ± 4.153	(12)	0.002[a]	15.348 ± 6.167	(12)	0.000[a]	10.165 ± 6.564	(15)	0.245[a]
B	10	M	GHR/BP +/+	3.248 ± 0.672	(15)		3.524 ± 1.705	(12)		6.688 ± 2.071	(12)		13.141 ± 7.140	(15)	
C	10	F	GHA	3.285 ± 0.547	(3)	0.010[b]	3.713 ± 1.988	(3)	0.003[b]	7.853 ± 0.965	(3)	0.005[b]			
D	10	F	NT	2.409 ± 0.263	(3)	0.876[c]	0.826 ± 0.087	(3)	0.062[c]	4.534 ± 0.403	(3)	0.109[c]			
						0.005[d]			0.191[d]			0.086[d]			
E	10	M	GHA	4.940 ± 0.920	(28)	0.000[e]	6.575 ± 2.484	(16)	0.000[e]	11.160 ± 3.047	(16)	0.000[e]	10.588 ± 2.918	(28)	0.963[e]
F	10	M	NT	2.436 ± 0.426	(39)	0.000[f]	3.090 ± 0.909	(12)	0.136[f]	5.676 ± 1.158	(12)	0.003[f]	10.552 ± 3.253	(39)	0.000[f]
						0.021[g]			0.001[g]			0.001[b]			0.000[g]
G	52	M	GHA	6.623 ± 2.766	(3)	0.127[h]	8.772 ± 6.946	(3)	0.022[h]	20.294 ± 5.816	(3)	0.025[h]	27.310 ± 8.207	(3)	0.437[h]
H	52	M	NT	3.452 ± 0.698	(3)		1.407 ± 0.597	(3)		8.159 ± 1.595	(3)		34.620 ± 2.180	(3)	
I	10	M	bGH	2.563 ± 0.321	(9)	0.594[i]	3.292 ± 0.669	(3)	0.348[i]	5.640 ± 1.087	(3)	0.143[i]	11.381 ± 2.555	(9)	0.071[i]
J	10	M	NT	2.646 ± 0.357	(11)		3.827 ± 0.746	(5)		6.678 ± 0.690	(5)		14.375 ± 4.059	(11)	

Note. R = normalized tissue weight; N = number of subjects; *P* = calculated by one-way ANOVA analysis (STATISTICAL).
[a] A vs B.
[b] C vs D.
[c] D vs F.
[d] C vs E.
[e] E vs F.
[f] F vs H.
[g] E vs G.
[h] G vs H.
[i] I vs J.

These data indicated that the enlargement of iBAT is most likely determined by age or via GH action rather than by gender. Two-way ANOVA also demonstrated a consistent difference ($P < 0.01$) between genotypes and age across iAT lobes, iBAT, and iWAT.

eWAT Increases with Age in Mice. Reduction of eWAT weights were statistically significant ($P < 0.01$) in GHA and GHR/BP$^{-/-}$ mice relative to their control animals at 10 weeks of age, but these reductions were not seen in normalized eWAT weights (Table III). Thus, the weight of eWAT appeared to be proportional to body weight across genotypes, as seen in most tissues other than iAT lobes in dwarf mice (data not shown). Two-way ANOVA also suggested that genotypes were not responsible for the reduction of normalized eWAT weights ($P = 0.416$), but were important for iBAT, iWAT, and iAT weights ($P < 0.01$). Furthermore, in both GHA and control mice, the normalized eWAT weights were significantly increased from 10 to 52 weeks of age, indicating that eWAT growth may increase with age and is not influenced by the GH signaling status of the animals.

Adipose Tissue Distribution of GHR/BP mRNAs in Male and Female Mice. Because expression of GHR and GHBP has not been reported in iBAT, we examined the status of GHR/BP mRNAs in iBAT, scWAT, gWAT (eWAT or oWAT), liver, and kidney in 10-week-old wild-type male and female mice.

Two forms of GHR/BP, a 4.5-kb band and a 1.2-kb band, were observed (Fig. 1). We and others (29) have shown that the higher molecular weight band represents GHR mRNA, whereas the lower band represents the GHBP mRNA. The 1.2-kb GHBP band was more intense than the 4.5-kb GHR band.

Expression Patterns of β-Actin in Mouse Tissues. Total RNA levels were normalized relative to the levels of 18S and/or 28S ribosomal RNAs across samples.

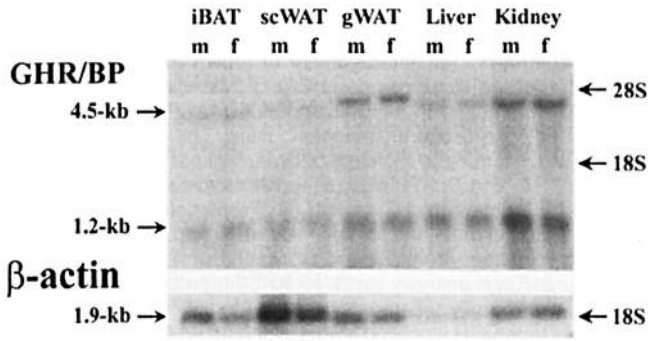

Figure 1. Northern analysis of GHR and GHBP in tissues from normal mice at 10 weeks of age. Total RNA samples (20 μg/lane) were prepared for Northern blotting from iBAT, scWAT, gWAT, liver, and kidney of 10-week-old male and female mice as described in "Materials and Methods." A 522-bp GHR/BP PCR Dig-labeled probe detected two isoforms of GHR transcripts after a 4-hr exposure; a 4.5-kb GHR band and a 1.2-kb GHBP band. The 1.2-kb band was generally more intense than the 4.5-kb band. A 540-bp β-actin PCR Dig-labeled probe detected a 1.9-kb band across tissues after a 1-hr exposure. The intensity volume's when ranked from high to low were liver, kidney, gWAT, iBAT, and scWAT.

Also, β-actin mRNA levels were used as an internal control in these studies. A 1.9-kb band was detected in iBAT, scWAT, gWAT, liver, and kidney (Fig. 1), in iBAT and eWAT (Fig. 2A), and in iBAT, iWAT, and eWAT (Fig. 3A) as reported (31). However, the intensity of the actin-specific bands varied. The intensity volumes of β-actin signals were ranked from low to high in the following order: liver, kidney, gWAT, iBAT, and scWAT (Fig. 1). The 1.9-kb band was more pronounced in eWAT than other adipose tissues (Figs. 2A and 3A). β-Actin levels increased 139%–146% for eWAT in both GHA and NT control mice between 10 to 52 weeks of age. Also, these levels for GHA eWAT were 60%–62% of NT eWAT at both 10 and 52 weeks of age. These data indicate that the levels of β-actin transcripts may increase as a function of age and may also vary as a function of GH signaling status of the animals.

An additional 1.4-kb band was detected using the same β-actin probe in iWAT (Fig. 3A) with different patterns of the 1.9- and 1.4-kb bands in iBAT or eWAT. There are at least two major muscle α-actin molecules: a 1.2-kb skeletal muscle isoform (32) and 1.3-kb vascular smooth muscle isoform (33). In our studies, it is unlikely that iWAT was contaminated by muscle isoforms because iWAT had a paler color and less abundant blood vessels than iBAT. These *in vivo* observations were contradictory to *in vitro* reports (34) and suggest that β-actin may be regulated differently *in vivo* and *in vitro*. As a component of the cytoskeleton, this difference may be an indicator of adipocyte development (34, 35).

The UCP1 Gene Is Negatively Regulated by GH-Mediated Signaling. Using a 605-bp UCP1 hybridiza-

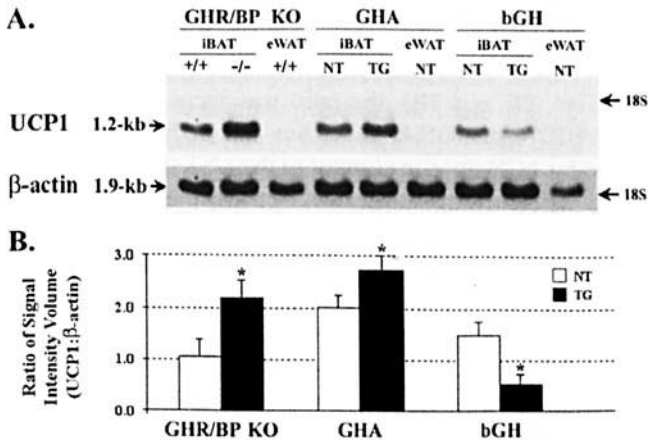

Figure 2. Northern analysis of UCP1 in transgenic mouse iBAT. Total RNA samples (20 μg/lane) were prepared from iBAT and eWAT of bGH, GHA, GHR/BP$^{-/-}$, and control mice at 10 weeks of age as described in "Materials and Methods." (A) UCP1 and β-actin. A 605-bp UCP1 PCR Dig-labeled probe detected a 1.2-kb band in iBAT but not in eWAT after a 2-hr exposure. This band is specific to iBAT. A 540-bp β-actin PCR Dig-labeled probe hybridized to a 1.9-kb band across iBAT and eWAT after a 24-hr exposure. (B) Ratio of signal intensity volume (UCP1:β-actin). This ratio was determined by the mean of duplicates ($n = 2$) as 2.05-fold higher in GHR/BP$^{-/-}$ ($P = 0.013$, $n = 2$), 1.35-fold higher in GHA ($P = 0.031$), and 0.32-fold lower in bGH ($P = 0.045$) mice relative to control littermates.

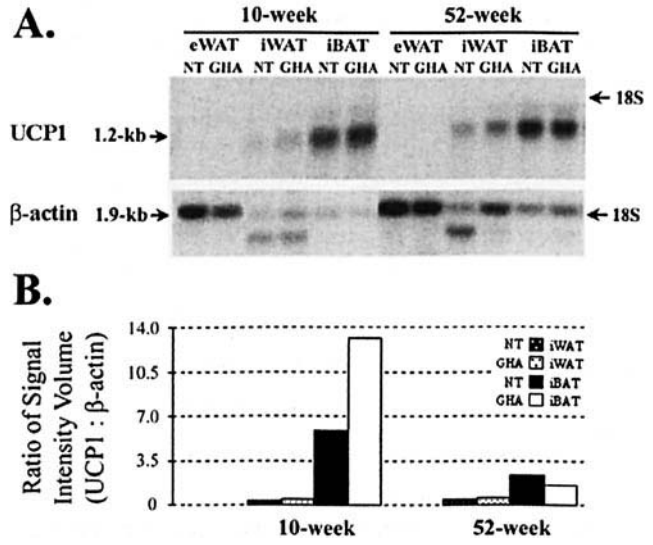

Figure 3. Northern blots of UCP1 in BAT from GH antagonist mice. Total RNA samples (50 μg/lane) were pooled from three of each iBAT, iWAT, and eWAT of GHA and NT mice at 10 or 52 weeks of age as described in "Materials and Methods." (A) UCP1 and β-actin. A 605-bp UCP1 ^{32}P-PCR-labeled probe detected a 1.2-kb band in iBAT and iWAT but not in eWAT after a 2-hr exposure. A 540-bp β-actin ^{32}P-PCR-labeled probe hybridized to a 1.9-kb band across all examined tissues after a 20-hr exposure. The 1.9-kb band was more pronounced in eWAT. An additional 1.4-kb band was also shown in iWAT, resulting in a different pattern of β-actin transcripts from iBAT to eWAT. (B) Ratio of signal intensity volume (UCP1:β-actin). This ratio was based on one run of pooled samples and determined to evaluate the relative level of UCP1 transcripts from tissue to tissue.

tion probe, we did not detect a signal in eBAT, bone, brain, heart, intestine, kidney, liver, lung, muscle, ovary, skin, spleen, scWAT, or testis (36). However, a strong signal was found in iBAT and iWAT (Figs. 2A and 3A). This was consistent with previous results (11) and demonstrates the skill of the surgeon in removing BAT. When the intensity volumes of UCP1 signals were normalized to those of β-actin (Figs. 2B and 3B), the ratio was increased 2-fold for GHR/BP$^{-/-}$ and GHA mice, but was reduced by about 3-fold for bGH mice in contrast to their NT littermates at 10 weeks of age. This suggested that GH might negatively regulate UCP1 gene expression.

Analysis of Brown Adipocytes Heterogeneity in iAT Lobes. iAT lobes consist of both iBAT and iWAT components. In iAT lobes, there is no clear interface between iBAT and iWAT. However, the iWAT component had a paler color and less abundant blood vessels than the iBAT component. During the total RNA preparation, we observed that the volume of the lipid varied from tissue to tissue after tissue preparation and centrifugation (data not shown). It increased qualitatively from marginal to enormous from iBAT (lowest), to iWAT (intermediate), and eWAT (highest).

To examine the heterogeneity of iBAT and iWAT in tissue preparations, the proportion of iBAT or iWAT weight in the iAT lobes was determined. An expansion of iWAT component in the iAT lobes was elevated in all mice relative to their NT littermates (Fig. 4). It was increased more in

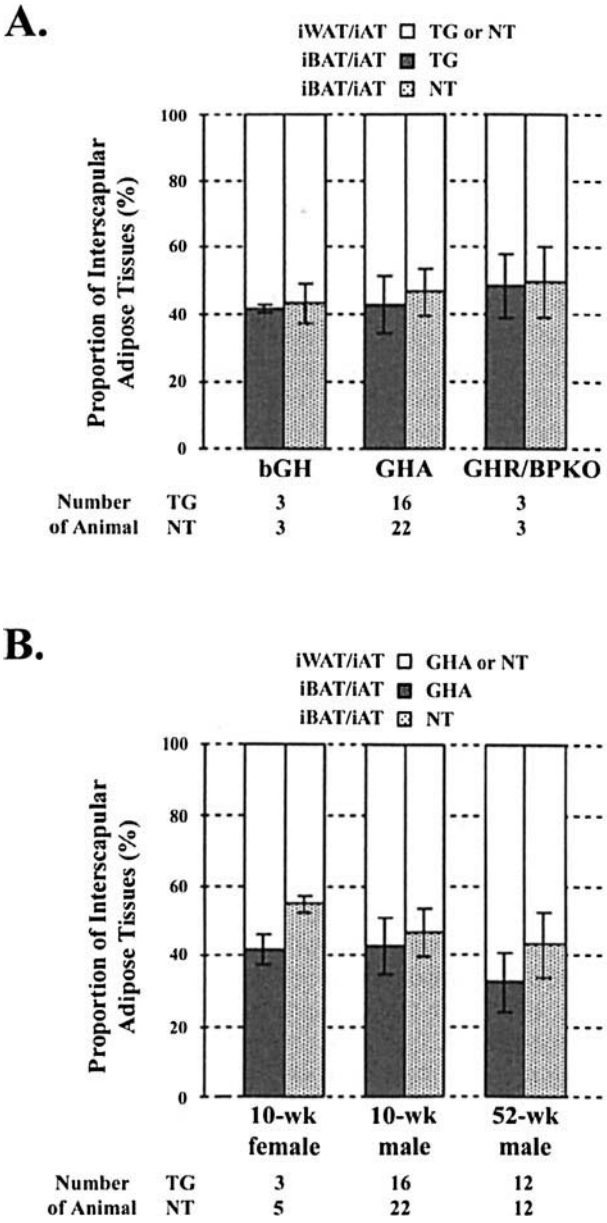

Figure 4. Analysis of heterogeneity of brown adipocytes in iAT. Mice were fed *ad libitum* as described in "Materials and Methods." iAT lobes were analyzed for iBAT and iWAT. (A) Proportion of interscapular adipose tissue in transgenic mice. The weight shift from iBAT to iWAT tended to increase between animal lines in the order of bGH, GHA, and GHR/BPKO, although no statistical change was observed in contrast to NT males. (B) Proportion of interscapular adipose tissue in male and female mice at 10 and 52 weeks of age. The shift increased from 10 and 52 weeks of age in GHA mice. Two-way ANOVA analysis revealed that the proportion of iBAT to iAT was significantly different across genders ($P < 0.05$) and was correlated to the GH signaling status of the mice. A moderate difference ($P = 0.089$) was also shown between GHA and NT mice at 10 to 52 weeks of age. Number of animals is indicated in Table III.

bGH mice relative to GHA and GHR/BP$^{-/-}$ animals (Fig. 4A). Also, this expansion was larger in GHA mice than in NT littermates between 10 to 52 weeks of age (Fig. 4B). Two-way ANOVA revealed that the heterogeneity of brown adipocytes in iAT is affected more by the GH signaling status ($P < 0.05$) than by age ($P = 0.089$) in both male and

female animals. The analysis also revealed an additive effect of age, GH signaling status, and gender in determining the composition of iBAT and iWAT in iAT lobes.

To further analyze the heterogeneity of brown adipocytes in iAT, we normalized UCP1 mRNA levels to β-actin RNA levels in all tissue and found that the ratio for iBAT UCP1 mRNA was reduced between 10 and 52 weeks of age (Fig. 3B). These normalized iBAT UCP1 mRNA levels were decreased to 12.1% for GHA and 39.2% for NT in 52-week-old mice in contrast to a slight increase of iWAT UCP1 mRNA (107% for GHA and 117% for NT) between 10 and 52 weeks of age. Thus, the level of UCP1 mRNA is reduced in iBAT as a function of age.

The normalized UCP1 mRNA level was lower in iWAT than that in iBAT (Fig. 3B). At 10 weeks of age, UCP1 mRNA levels in iWAT were 3.7% in GHA mice and 5.7% in NT littermates as compared with the levels in iBAT. However, these percentages increased to 32.9% in GHA mice and 17.0% in NT littermates at 52 weeks of age. Thus, iWAT contains more UCP1-expressing adipocytes as a function of age, particularly in GHA iWAT.

We also consistently observed that the UCP1 mRNA levels were different between GHA mice and NT littermates (Fig. 3B). The normalized UCP1 mRNA levels were enhanced to 223% for iBAT and 145% for iWAT in GHA mice at 10 weeks of age, but were reduced to 68.6% for iBAT despite an increase to 132% for iWAT in GHA mice at 52 weeks of age. Expression of the UCP1 gene is enhanced in young GHA mice as seen in Figure 2A. However, this increase slowed and reversed in GHA iBAT as a function of age until the levels in GHA iBAT were similar to those found in NT iBAT at 52 weeks of age. The possibility that a loss of GHA iBAT UCP1 mRNA may be compensated by a gain of GHA iWAT UCP1 mRNA cannot be excluded.

Discussion

GH transgenic mice are larger, whereas GHA transgenic mice and GHR/BPKO mice are smaller than control animals. In our previous study (30), we showed that food intake was found to be proportional to body size in GHA, bGH, and NT littermates during the period of rapid postweaning growth. The feed efficiencies (gain/feed) and growth rates of GHA mice were similar to those of NT mice, whereas those of bGH mice were significantly increased. In this paper, we have demonstrated that GHA mice "catch up" with the NT littermates in body weight (Table II) but not in body length when mice age. Thus, normalizing body weight to body length, the aged GHA animal possesses a greater BMI than NT littermates. The higher BMI with an unchanged feed efficiency implies a shift in energy homeostasis in these GHA obese mice. It has been reported that an impairment of GH signaling causes obesity-prone rats to be more susceptible to obesity (37). These obesity effects are also found in the GHA mice that had higher body fat percentage and lower body protein percentage than NT littermates ($P < 0.05$) (30).

GH-mediated signaling is not completely understood in BAT. The presence of GHR has been suggested in BAT because GH inhibits malic enzyme and glucose-6-phosphate dehydrogenase, two enzymes that generate NADPH for lipogenesis (38). GHR and GHBP mRNAs have not been demonstrated in BAT, although their mRNAs were detected in different rat WAT depots and isolated adipocytes as well as adipocyte precursor cells (39). In this study, we have found that GHR and GHBP mRNAs were present in mouse BAT (Fig. 1). Thus, a reasonable generalization is that GH signaling occurs in BAT as it takes place in many other tissues, such as liver and muscles.

The role of GHBP in obesity etiology cannot be neglected because it serves complex functions, including buffering the circulating GH, prolonging plasma GH half-life, and competing with GHR for GH (40). Therefore, it is difficult to ascertain the net *in vivo* effect of GHBP, it may enhance and/or inhibit GH action. In this study, we do not know relative levels of serum GHBP and GHBP expression in adipose tissues in the three mouse models.

In the "GH-fat cycle" model (2), GH is postulated to stimulate lipolysis in various fat tissues. Free fatty acids (FFAs) released from adipocytes are likely to be metabolized within nearby cells and can also enhance the activity of UCPs. Interestingly, we have found abnormally enlarged iAT lobes in young GHA and GHR/BPKO mice (Table III). Northern analyses (Figs. 2 and 3) revealed that the levels of UCP1 transcripts were elevated in young GHA and GHR/BPKO iBAT in contrast to NT littermates and were reduced in young bGH iBAT. We postulate that GH action is intimately involved in control of the mass of iAT. GH stimulates lipolysis under normal conditions. In dwarf animals, GH signaling-mediated lipolysis is eliminated. The decrease of lipolysis results in a compensatory increase of BAT mass that likely maintains energy homeostasis in dwarf mice. One mechanism to account for the phenotypic effects is by upregulation of UCP1 gene expression. In the dwarf mice used in these studies, UCP-1 gene expression is elevated. On the other hand, overexpression of bGH may enhance GH signaling-mediated lipolysis that is likely responsible for the downregulation of UCP1 gene expression to maintain energy balance in these giant mice. Indeed, GH signaling negatively regulates UCP1 expression at a transcriptional level.

Because these phenotypic changes are seen in iBAT of GHA mice, we have used a two-way subtractive hybridization assay and have identified genes that are differentially expressed between the dwarf mice and controls (Li Y *et al.*, unpublished data). We have found two downregulated genes in GHA iBAT: adipocyte lipid-binding protein (aP2) and medium chain fatty acyl-coenzyme A dehydrogenase (FADH); three downregulated mitochondrial genes encoding cytochrome b and cytochrome c oxidase, as well as NADH-ubiquinone oxidoreductase; and three upregulated

genes that encode α-enolase and glucophosphate isomerase as well as pyruvate kinase. We postulate that these downregulated GHA iBAT genes may result in a deficit of energy consumption that is compensated by upregulation of the UCP1 gene and other GHA iBAT genes. For example, a reduced level of aP2 gene expression in GHA iBAT may result in a decreased subcellular concentration of FFAs that normally promote proton conductance by activating UCP1 and that is routinely metabolized by FADH in the mitochondria. A recent microarray study illustrated that genes involved in β-oxidation of FFAs are developmentally coregulated with UCP1 (13).

Although BAT disappears in adult primates, a large proportion of brown adipocytes were found in baboon adipose tissues upon cold exposure (41), suggesting heterogeneity of adipocytes in fat pads. In this regard, brown adipocytes can be found not only in BAT, but also in WAT (8). It has also been reported that UCP1 was reduced in intraperitoneal WAT in morbidly obese patients in contrast to lean controls, further suggesting that WAT contains brown adipocytes (42). Here, we observed a reduction of UCP1 expression in GHA iBAT and an elevation of UCP1 expression in GHA iWAT as a function of age.

BAT and WAT may be interconvertible and they represent two extreme ends of a continuous spectrum of adipose tissue (43). It was reported that UCP1 rapidly disappeared from various BAT depots after birth in cows and sheep (44). On the other hand, UCP1 and LPL mRNAs in mouse inguinal WAT were detected and the amount of developed mitochondria UCP1 in cold-stressed inguinal adipocytes tended to be equal to that of primary mitochondria UCP1 in brown adipocytes (45). BAT-like changes of UCP1 expression were also demonstrated with increases of brown adipocyte number and mitochondrial cristae density after cold exposure to rat periovarian WAT (46). Thus, a third type of adipose tissue has been proposed: convertible adipose tissue (CAT) (47). It was hypothesized that the interchangeability of BAT and WAT may be determined by many transcription factors (TFs) in adipose stem cells, such as peroxisome proliferator-activated receptor γ (PPARγ) (48), CAAT/enhancing binding proteins (C/EBPs) (49), adipocyte determination and differentiation factor-1 (ADD1) (50), PPARγ coactivator-1 (PGC-1) (51), and preadipocyte factor-1 (Pref-1) (52). However, the mechanism of differentiation and proliferation of adipocytes remains unclear.

In summary, iAT normally grows and enlarges as a function of age, but this enlargement occurs abnormally in genetically modified dwarf mice. These dwarf mice possess an enlarged BAT. Hence, we concluded that GH-mediated signaling plays an important role in BAT metabolism and body weight regulation. Because GH-mediated signaling negatively regulates the expression of UCP1 in iAT, we proposed that decreased levels of GH signaling may lead to abnormal BAT development that may affect many differentially expressed genes (36). We expect that aberrant GH signaling would cause a change of brown adipocyte size and number as well as function in both dwarf and giant mice. The regulatory mechanism of GH signaling on UCP1 expression and physiological significance will be the subject of future studies.

We thank Dr. Leslie P. Kozak for the gift of UCP1 plasmid, Dr. Karen Coschigano for providing technical expertise in RNA isolation and analyses, Dr. Linda L. Bellush and Amy N. Holland for maintaining the breeding colonies of mice, and Marcus Rider for photography.

1. Goodman HM. Growth hormone and metabolism. In: Schreibman MP, Scanes CG, Pang PKT, Eds. The Endocrinology of Growth, Development, and Metabolism in Vertebrates. San Diego: Academic Press, pp93–115, 1993.
2. Gertner JM. Growth hormone actions on fat distribution and metabolism. Horm Res **38**:41–43, 1992.
3. Veldhuis JD, Iranmanesh A, Ho KK, Waters MJ, Johnson ML, Lizarralde G. Dual defects in pulsatile growth hormone secretion and clearance subserve the hyposomatotropism of obesity in man. J Clin Endocrinol Metab **72**:51–59, 1991.
4. Johannsson G, Marin P, Lonn L, Ottosson M, Stenlof K, Bjorntorp P, Sjostrom L, Bengtsson BA. Growth hormone treatment of abdominally obese men reduces abdominal fat mass, improves glucose and lipoprotein metabolism, and reduces diastolic blood pressure. J Clin Endocrinol Metab **82**:727–734, 1997.
5. Roemmich JN, Huerta MG, Sundaresan SM, Rogol AD. Alternations in body composition and fat distribution in growth hormone-deficient prepubertal children during growth hormone therapy. Metabolism **50**:537–547, 2001.
6. Richelsen B, Pedersen SB, Kristensen K, Borglum JD, Norrelund H, Christiansen JS, Jorgensen JO. Regulation of lipoprotein lipase and hormone-sensitive lipase activity and gene expression in adipose and muscle tissue by growth hormone treatment during weight loss in obese patients. Metabolism **49**:906–911, 2000.
7. Dietz J, Schwartz J. Growth hormone alters lipolysis and hormone-sensitive lipase activity in 3T3-F442A adipocytes. Metabolism **40**: 800–806, 1991.
8. Himms-Hagen J. Brown adipose tissue thermogenesis: interdisciplinary studies. FASEB J **4**:2890–2898, 1990.
9. Cornelius P, MacDougald OA, Lane MD. Regulation of adipocyte development. Annu Rev Nutr **14**:99–129, 1994.
10. Arbuthnott E. Brown adipose tissue: structure and function. Proc Nutr Soc **48**:177–182, 1989.
11. Kozak LP, Britton JH, Kozak UC, Wells JM. The mitochondrial uncoupling protein gene. Correlation of exon structure to transmembrane domains. J Biol Chem **263**:12274–12277, 1988.
12. Nibbelink M, Moulin K, Arnaud E, Duval C, Pénicaud L, Casteilla L. Brown fat UCP1 is specifically expressed in uterine longitudinal smooth muscle cells. J Biol Chem **276**:47291–47295, 2001.
13. Master SR, Hartman JL, D'Cruz CM, Moody SE, Keiper EA, Ha SI, Cox JD, Belka GK, Chodosh LA. Functional microarray analysis of mammary organogenesis reveals a developmental role in adaptive thermogenesis. Mol Endocrinol **16**:1185–1203, 2002.
14. Lowell BB, Susulic V, Hamann A, Lawitts JA, Himms-Hagen J, Boyers BB, Kozak LP, Flier JS. Development of obesity in transgenic mice after genetic ablation of brown adipose tissue. Nature **366**:740–742, 1993.
15. Kopecky J, Clarke G, Enerback S, Spiegelman B, Kozak LP. Expression of the mitochondrial uncoupling protein gene from the aP2 gene promoter prevents genetic obesity. J Clin Invest **96**:2914–2923, 1995.
16. Enerback S, Jacobsson A, Simpson EM, Guerra C, Yamashita H, Harper ME, Kozak LP. Mice lacking mitochondrial uncoupling protein are cold-sensitive but not obese. Nature **387**:90–94, 1997.
17. Kozak LP, Koza RA. Mitochondria uncoupling proteins and obesity:

molecular and genetic aspects of UCP1. Int J Obes Relat Metab Disord **23**(Suppl 6):S33–S37, 1999.
18. Fleury C, Neverova M, Collins S, Raimbault S, Champigny O, Levi-Meyrueis C, Bouillaud F, Seldin MF, Surwit RS, Ricquier D, Warden CH. Uncoupling protein-2: a novel gene linked to obesity and hyperinsulinemia. Nat Genet **15**:269–272, 1997.
19. Vidal-Puig A, Solanes G, Grujic D, Flier JS, Lowell BB. UCP3: an uncoupling protein homologue expressed preferentially and abundantly in skeletal muscle and brown adipose tissue. Biochem Biophys Res Commun **235**:79–82, 1997.
20. Mao W, Yu XX, Zhong A, Li W, Brush J, Sherwood SW, Adams SH, Pan G. UCP4, a novel brain-specific mitochondrial protein that reduces membrane potential in mammalian cells [published erratum appears in FEBS Lett 449:293, 1999]. FEBS Lett **443**:326–330, 1999.
21. Pedersen SB, Kristensen K, Fisker S, Jorgensen JOL, Christiansen JS, Richelsen B. Regulation of uncoupling protein-2 and -3 by growth hormone in skeletal muscle and adipose tissue in growth hormone-deficient adult. J Clin Endocrinol Metab **84**:4073–4078, 1999.
22. Pedersen SB, Borglum JD, Kristensen K, Norrelund H, Otto J, Jorgensen L, Richelsen B. Regulation of uncoupling protein (UCP) 2 and 3 in adipose and muscle tissue by fasting and growth hormone treatment in obese humans. Int J Obes Relat Metab Disord **24**:968–975, 2000.
23. Chen WY, Wight DC, Wagner TE, Kopchick JJ. Expression of a mutated bovine growth hormone gene suppresses growth of transgenic mice. Proc Natl Acad Sci U S A **87**:5061–5065, 1990.
24. Chen WY, White ME, Wagner TE, Kopchick JJ. Functional antagonism between endogenous mouse growth hormone (GH) and a GH analog results in dwarf transgenic mice. Endocrinology **129**:1402–1408, 1991.
25. Chen WY, Wight DC, Mehta BV, Wagner TE, Kopchick JJ. Glycine 119 of bovine growth hormone is critical for growth-promoting activity. Mol Endocrinol **5**:1845–1852, 1991.
26. Chen WY, Wight DC, Chen NY, Coleman TA, Wagner TE, Kopchick JJ. Mutations in the third α-helix of bovine growth hormone dramatically affect its intracellular distribution in vitro and growth enhancement in transgenic mice. J Biol Chem **266**:2252–2258, 1991.
27. Chen WY, Chen N, Yun J, Wagner TE, Kopchick JJ. In vitro and in vivo studies of the antagonistic effects of human growth hormone analogs. J Biol Chem **269**:15892–15897, 1994.
28. Chen WY, Chen NY, Yun J, Wight DC, Wang XZ, Wagner TE, Kopchick JJ. Amino acid residues in the third alpha-helix of growth hormone involved in growth promoting activity. Mol Endocrinol **9**: 292–302, 1995.
29. Zhou Y, Xu BC, Maheshwari HG, He L, Reed M, Lozykowski M, Okada S, Cataldo L, Coschigamo K, Wagner TE, Baumann G, Kopchick JJ. A mammalian model for Laron syndrome produced by targeted disruption of the mouse growth hormone receptor/binding protein gene (the Laron mouse). Proc Natl Acad Sci U S A **94**:13215–13220, 1997.
30. Knapp JR, Chen WY, Turner ND, Byers FM, Kopchick JJ. Growth patterns and body composition of transgenic mice expressing mutated bovine somatotropin genes. J Anim Sci **72**:2812–2819, 1994.
31. Tokunaga K, Taniguchi H, Yoda K, Shimizu M, Sakiyama S. Nucleotide sequence of a full-length cDNA for mouse cytoskeletal beta-actin mRNA. Nucleic Acids Res **14**:2829, 1986.
32. Minty AJ, Caravatti M, Robert B, Cohen A, Daubas P, Weydert A, Gros F, Buckingham ME. Mouse actin messenger RNAs. Construction and characterization of a recombinant plasmid molecule containing a complementary DNA transcript of mouse α-actin mRNA. J Biol Chem **256**:1008–1014, 1981.
33. Min BH, Strauch AR, Foster DN. Nucleotide sequence of a mouse vascular smooth muscle α-actin cDNA. Nucleic Acids Res **16**:10374, 1988.
34. Gaskins HR, Kim JW, Hausman GJ. Decreases in local hormone biosynthesis and c-fos gene expression accompany differentiation of porcine preadipocytes. In Vitro Cell Dev Biol **26**:1049–1056, 1990.
35. O'Shea Alvarez MS. 3T3 cells in adipocytic conversion. Arch Invest Med (Mex) **22**:235–244, 1991.
36. Li Y, Kelder B, Kopchick JJ. Identification, isolation, and cloning of growth hormone (GH)-inducible interscapular brown adipose complementary deoxyribonucleic acid from GH antagonist mice. Endocrinology **142**:2937–2945, 2001.
37. Lauterio TJ, Barkan A, DeAngelo M, DeMott-Friberg R, Ramirez R. Plasma growth hormone secretion is impaired in obesity-prone rats before onset of diet-induced obesity. Am J Physiol **275**:E6–E11, 1998.
38. Carvalho SD, Negrao N, Bianco AC. Hormonal regulation of malic enzyme and glucose-6-phosphate dehydrogenase in brown adipose tissue. Am J Physiol **264**:E874–E881, 1993.
39. Vikman K, Carlsson B, Billig H, Eden S. Expression and regulation of growth hormone (GH) receptor messenger ribonucleic acid (mRNA) in rat adipose tissue, adipocytes, and adipocyte precursor cells: GH regulation of GH receptor mRNA. Endocrinology **129**:1155–1161, 1991.
40. Baumann G. Growth hormone binding protein 2001. J Pediat Endocrinol **14**:355–375, 2001.
41. Viguerie-Bascands N, Bousquet-Melou A, Galitzky J, Larrouy D, Ricquier D, Berlan M, Casteilla L. Evidence for numerous brown adipocytes lacking functional β3-adrenoceptors in fat pads from nonhuman primates. J Clin Endocrinol Metab **81**:368–375, 1996.
42. Oberkofler H, Dallinger G, Liu YM, Hell E, Krempler F, Patsch W. Uncoupling protein gene. quantification of expression levels in adipose tissues of obese and non-obese humans. J Lipid Res **38**:2125–2133, 1997.
43. Ashwell W. Is there a continuous spectrum of the adipose tissues in animal and man? In: Vague J, Bjorntorp B, Guy-Grand M, Rebuffe-Srive, Vague P, Eds. Metabolic Complications of Human Obesities. New York: Elsevier Science Publishers, pp265–274, 1985.
44. Ailhaud G, Grimaldi P, Negrel R. Cellular and molecular aspects of adipose tissue development. Annu Rev Nutr **12**:207–233, 1992.
45. Loncar D. Convertible adipose tissue in mice. Cell Tissue Res **266**:149–161, 1991.
46. Cousin B, Cinti S, Morroni M, Raimbault S, Ricquier D, Penicaud L, Casteilla L. Occurrence of brown adipocytes in rat white adipose tissue: molecular and morphological characterization. J Cell Sci **103**: 931–942, 1992.
47. Loncar D, Bedrica L, Mayer J, Cannon B, Nedergaard J, Afzelius BA, Svajger A. The effect of intermittent cold treatment on the adipose tissue of the cat. Apparent transformation from white to brown adipose tissue. J Ultrastruct Mol Struct Res **97**:119–129, 1986.
48. Tontonoz P, Hu E, Graves RA, Budavari AI, Spiegelman BM. mPPARγ2: tissue-specific regulator of an adipocyte enhancer. Genes Dev **8**:1224–1234, 1994.
49. Mandrup S, Lane MD. Regulating adipogenesis. J Biol Chem **272**: 5367–5370, 1997.
50. Tontonoz P, Kim JB, Graves RA, Spiegelman BM. ADD1: a novel helix-loop-helix transcription factor associated with adipocyte determination and differentiation. Mol Cell Biol **13**:4753–4759, 1993.
51. Spiegelman BM, Puigserver P, Wu Z. Regulation of adipogenesis and energy balance by PPARγ and PGC-1. Int J Obes Relat Metab Disord **24**(Suppl 4):S8–S10, 2000.
52. Sul HS, Smas C, Mei B, Zhou L. Function of pref-1 as an inhibitor of adipocyte differentiation. Int J Obes Relat Metab Disord **24**(Suppl 4):S15–S19, 2000.